

## Simulation of disk- and band-like voids in dusty plasma systems

Y. H. Liu

*Department of Chemistry, University of Antwerp, Universiteitsplein 1, B-2610 Antwerp, Belgium  
and Institute of Physics, Chinese Academy of Sciences, 100080 Beijing, People's Republic of China*

Z. Y. Chen<sup>a)</sup>

*Department of Chemistry, University of Antwerp, Universiteitsplein 1, B-2610 Antwerp, Belgium*

F. Huang

*College of Science, China Agricultural University, 100083 Beijing, People's Republic of China*

M. Y. Yu

*Theoretische Physik I, Ruhr-Universität Bochum, D-44780 Bochum, Germany*

L. Wang

*Institute of Physics, Chinese Academy of Sciences, 100080 Beijing, People's Republic of China*

A. Bogaerts

*Department of Chemistry, University of Antwerp, Universiteitsplein 1, B-2610 Antwerp, Belgium*

(Received 19 December 2005; accepted 10 April 2006; published online 12 May 2006)

The minimum-energy configurations of systems of multispecies charged grains of different mass and charge with an interaction potential including long-range repulsive as well as short-range attractive components are studied by molecular dynamics simulation. The grains are also subject to a radial drag force and a quadratic confining potential. It is found that central as well as band-like void regions separating grains of different species can exist as well as coexist, depending on the species parameters. The results are consistent with the horizontal cross-sections of the structures found in a recent experiment on self-organization of chemically synthesizing grains [Huang *et al.* *Chin. Phys. Lett.* **21**, 121 (2004)]. © 2006 American Institute of Physics.

[DOI: [10.1063/1.2201058](https://doi.org/10.1063/1.2201058)]

### I. INTRODUCTION

The phenomena of voids, or local dust-free regions, in dust containing plasmas have recently attracted much attention.<sup>1-14</sup> Laboratory observations suggest that the void configuration is fairly robust and independent of the initial processes triggering it. A void in the dust cloud usually has a sharp boundary. In general, the void size increases with rf power input and the neutral gas pressure. The appearance of a void can be considered as the result of local evacuation of the dust grains by a balance of the forces acting on them. Several mechanisms have been proposed and studied,<sup>2-13</sup> but a complete theory is still lacking. Besides the external forces (such as that of the confining electric and/or magnetic fields), possible forces on the dust grains include thermophoretic, space-charge, ion-drag (since the ions are streaming towards the walls), as well as other collisional forces. Several theories also invoke ionization or other effects for triggering void formation.<sup>7-10</sup> The ubiquitous sharp boundary of the void has been attributed to a limitation of the spatial locations where the delicate force balance can take place.<sup>11</sup> However, dust-containing plasma systems are inherently complex since many effects are closely related and can interact with each other. It is thus difficult to differentiate them in attempts to pinpoint the main mechanisms for void formation.<sup>2-6,8,10,11</sup>

Most investigations on voids concern dusty-plasma sys-

tems in equilibrium or near equilibrium, where the dust grains are no longer evolving. For *in situ* chemically synthesized dust grains, well before the final stage of the grain evolution, the dust grains are very fine and weakly charged. The electrochemically evolving system, containing grains of many species with different mass, charge, physical shape, and perhaps also chemical composition, is physically rather complex. Furthermore, at this stage the intergrain distance (in the dust containing region) is smaller than or similar to that of the plasma Debye length. It is also not certain how the grains interact with each other in the presence of the background plasma and neutral particles. Nevertheless, in a recent experiment,<sup>14</sup> in which the grains are still being chemically synthesized, well-defined single as well as concentric multiple shell- or dome-like voids, separated by shells of dust grains (of different sizes, when distinguishable), were observed at various times of the evolution of the still very fine dust grains. For example, a central dome void may first appear, and after some minutes a shell-like void appears enclosing the central dome void.

In this paper, we investigate by means of molecular dynamics (MD) simulation the formation of two-dimensional (2D) disk- and band-like voids of a multispecies dust system.<sup>3,14</sup> For simplicity, we shall consider plasmas containing up to several species of dust grains with different mass and charge interacting through the Coulomb potential. To simulate the effect of the background plasma as well as the close-neighbor dust grains, we also assume that the inter-

<sup>a)</sup>Present address: Department of Chemistry, George Washington University, Washington, DC 20052.

grain interaction potential contains an attractive component.<sup>3,6,15–19</sup> The system is located in a radially symmetric quadratic potential.<sup>20–24</sup> A radially outward drag force on the grains, simulating the drag of the ions streaming to the plasma boundary, is also included. The MD simulation starts with a random (thermal) grain distribution and ends when a quasistationary or minimum-energy state is reached. Thus, if there is only one species of dusts, only the central disk-like void can be expected. The investigation should also be applicable to some three-dimensional (3D) systems in which the dust grains are localized in different 2D horizontal planes in crystal-like layers. Our result qualitatively agrees with the experimental observations of Huang *et al.*<sup>14</sup> It also suggests that in the experiments of void formation, one can obtain additional information about the physics involved by adding a new species of dust grains.<sup>23</sup>

## II. MODEL SYSTEM

In the existing literature, the dust-dust interaction is usually assumed to be governed by a screened Coulomb potential.<sup>2–6,8,10</sup> However, here we are concerned with a dusty plasma system in the early or middle stages of evolution. That is, the dust grains are still growing slowly, namely on the chemical or aggregation time scale, as compared to the dust-dynamic, or self-organization, time scale involved in their self-organization. In fact, in the experiments of Huang *et al.*,<sup>14,25</sup> the dome- and/or shell-like voids can only be observed (lasting about 20 min) during the system evolution. After the grains become bigger and clearly distinguishable, the voids disappear and the normal plasma-crystal structure emerges.<sup>25</sup> It is at present still uncertain how significant is the Debye screening effect, if any, of the still-evolving weakly charged fine dust grains. On the other hand, it is clear that the cohesive effect of the background plasma and neutral particles on the grains can affect the latter's interaction dynamics.<sup>6,3</sup> Therefore, in our MD simulation we shall assume a grain-grain interaction potential consisting of a pure Coulomb repulsive potential with a short-range attractive component.

We consider a system of charged grains interacting through a potential containing a long-range (Coulomb) repulsive and a short-range attractive component.<sup>15,17–19</sup> The grains are externally confined by a quadratic potential, centered at the origin and increasing radially as  $r^2$ . Such a potential can represent an external confinement field or the effect of a rotating system.<sup>20–24</sup> An external force, representing the drag force on a dust grain of the ions streaming to the plasma boundary, is also included. In the dimensionless form, the Hamiltonian of the system is  $H=K+U$ , where  $K$  is the kinetic energy and

$$U = \sum_{i=1}^N (m_i^{(k)} r_i^2 - A q_i^{(k)2} r_i) + \sum_{i<j}^N q_i^{(k)} q_j^{(k)} \times \left( \frac{1}{|\mathbf{r}_i - \mathbf{r}_j|} - B e^{-\kappa|\mathbf{r}_i - \mathbf{r}_j|} \right) \quad (1)$$

is the potential energy. In Eq. (1), the first term is the confinement potential,<sup>20–24</sup> the second is the potential associated

with the drag force,<sup>5,6</sup> and the third and last are the repulsive and attractive parts of the interparticle potential, respectively.<sup>3,6,16–19</sup> Here,  $N = \sum_{k=1}^n N^{(k)}$  is the total number of grains, where  $n$  is the total species number in the system, and  $N^{(k)}$  is the number of the grain species  $k$ . The parameter  $A$  determines the strength of the drag force, and  $B$  and  $\kappa$  determine the strength and the interaction range of the attractive part of the intergrain potential, respectively,  $\mathbf{r}_i$  is the position of the grain  $i$  ( $=1, \dots, N$ ),  $q_i^{(k)}$  and  $m_i^{(k)}$  are the dimensionless charge [normalized by  $Q^{(1)}$ ] and mass [normalized by  $M^{(1)}$ ] of the grain  $i$  of species  $k$ , and  $Q^{(1)}$  and  $M^{(1)}$  are the charge and the effective mass of species 1, respectively. Since the grains of the same species are indistinguishable, without loss of generality one can drop the grain indices on  $q_i^{(k)}$  and  $m_i^{(k)}$ . In Eq. (1), the units for the length and energy are  $r_0 = (2Q^{(1)2}/M^{(1)}\epsilon\omega_0^2)^{1/3}$  and  $E_0 = M^{(1)}\omega_0^2 r_0^2/2$ , respectively, where  $\omega_0$  is the trapping frequency, and  $\epsilon$  (constant) is the dielectric constant of the background electron-ion plasma. In the minimum-energy state, we have  $H \rightarrow U$ .

It should be mentioned that in evolution stage of interest here, the size, mass, as well as charge of dust grains are continuously changing by chemical reactions as well as aggregation. However, the time scale of such changes is much smaller than that of the dust dynamics. Thus, in our model we can assume that the size, mass, and charge of a dust grain remain constant.

We shall use MD simulation to follow the evolution of the grain system. Each run is started with a random phase-space distribution of the grains at a high temperature ( $T=0.05 \rightarrow 1.0$ , where  $T$  has been normalized by  $E_0$ ). The system is then slowly annealed until the quasistationary or minimum-energy state with temperature  $T \sim 0 \pm 10^{-6}$  is reached. The accuracy of the simulation was verified by reproducing the ground-state configurations of the single-species clusters of Nelissen *et al.*<sup>17</sup> obtained using the Monte-Carlo method. From Ref. 17, one sees that in monodisperse systems without any drag force, the grains organize themselves into rings around the trap center when  $B \sim 6.0$  and  $\kappa \sim 4.0$ . It is thus convenient to set  $B=6.0$  and  $\kappa=4.0$  in our investigation of multispecies systems.

## III. SIMULATION RESULTS

We shall first study the minimum-energy structure of a system ( $N=250$ ) with two species of grains with different charge and/or mass. We then consider a larger system ( $N=500$ ) with four species of grains.

### A. System with two species of grains

#### 1. Different mass

Figure 1 shows typical calculated minimum-energy configurations of a system ( $N=250$ ) with two species of grains having the same charge but different mass. In order to compare with a single-species system, the special case of  $m^{(2)} = m^{(1)} = 1.0$  is also included. In Fig. 1, the subfigures (all of the same arbitrary scale) are arranged such that the columns show the effect of the strength of the drag force  $A$ , and the rows show the effect of the relative mass  $m^{(2)}$ . Figures 1 (a1)–(a4) (the first column) are for  $m^{(2)} = m^{(1)} = 1.0$ , i.e., the

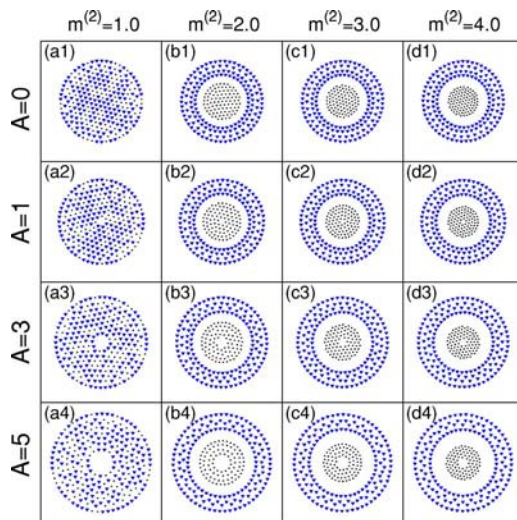


FIG. 1. (Color online) Calculated minimum-energy configurations for two-species grains of the same charge but different masses. The total number of grains is  $N=250$ . The numbers of grains of species 1 (triangles) and 2 (circles) are  $N^{(1)}=161$  and  $N^{(2)}=89$ , respectively.

species are physically indistinguishable. We see that with increasing  $A$ , a void appears at the center of the trap. As expected, the sizes of the void and the overall dust system increase with  $A$ , since with increasing  $A$ , the (outward) drag force is increased, but the mass-dependent (inward) confinement force is not.

From Figs. 1 (b2)–(d4), one can see that when  $m^{(2)} \neq m^{(1)} (=1.0)$ , grains of different species populate different shells, with those of the larger mass closer to the center of the trap. The shells have sharp boundaries, with a well-defined band-shaped void between them. Separation of the two species occurs since for a given  $A$ , the heavier grains suffer a stronger confinement force and are pushed towards the center of the trap, leaving the lighter grains behind and causing the appearance of a gap, or void. The overall configuration of the grain packing is of course determined by a static (ignoring the very weak fluctuations) minimum-energy balance among the external and grain-grain interaction forces in the minimum-energy state, with the repulsive Coulomb force preventing the grains from collapsing together. From Fig. 1, we also see that for a given  $m^{(2)}$ , with increasing  $A$  a void appears at the center of the trap. The sizes of the band-like void, the center void, as well as the overall system increase. These results can again be understood in terms of the competition of the drag and the confinement forces on the grains.

From Fig. 1, we also see that for a given  $A$ , with increasing  $m^{(2)}$  the size of the system almost does not change, but the shell formed by the heavier species-2 grains becomes more compact, and the size of the center void becomes smaller. The shell size of the lighter species-1 grains is, however, not changed, so that the size of the band void effectively increases with  $m^{(2)}$ . This result is due to the fact that at a given  $A$ , with increasing  $m^{(2)}$  the confinement force on the species-2 grains becomes stronger, so that the grains are pushed closer to the center of the trap, making the species-2 shell as well as the center void more compact. On the other

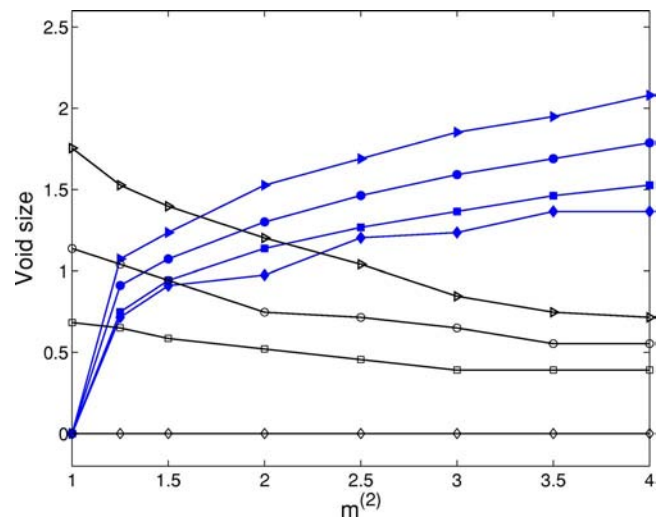


FIG. 2. (Color online) Calculated size dependence of the disk (open symbols) and band (solid symbols) voids on the species-2 mass for a drag strength  $A=0$  (diamond), 1 (square), 3 (circle), and 5 (triangle). The void size (radius for the disk voids and width for the band voids) is normalized by  $r_0$ . Note that even for  $A=0$ , band but no disk voids can appear.

hand, the confinement and drag forces on the species-1 grains are unchanged. Thus, the size of the species-1 shell remains almost constant. The thickness of the band void between the species-1 and 2 shells then increases with  $m^{(2)}$  since the size of the system is determined by the species-1 shell, which remains unchanged as  $m^{(2)}$  increases.

Figure 2 shows more quantitatively the variation of the void size with respect to  $m^{(2)}$  for different drag strengths ( $A$ ) in a plasma containing two dust species with different mass but the same charge. One can clearly see that as  $m^{(2)}$  increases, the center disk void decreases but the band void increases in size. The rate of variation depends on the drag strength  $A$ . As expected, the size of both the disk and band voids tends to saturate when  $m^{(2)}$  becomes large. We also note that even when there is no drag force ( $A=0$ ), band (but no disk) voids can appear.<sup>17</sup> One can understand these results by noting that in Eq. (1), the first and second terms together represent a displaced harmonic potential, like the ring-confinement potential of Schweigert *et al.*<sup>26</sup> for each species. In the displaced potential well, the minimum is not at the system center  $r=0$ , but at a radius of  $r=r_*$ , i.e., the potential supports a central void of radius  $r_*$  in the system. For the multispecies system, from the derivative  $\partial_r[(m^{(k)}r_*^{(k)})^2 - Aq^{(k)2}r_*^{(k)}]=0$ , we can obtain the critical radius  $r_*^{(k)}=A(q^{(k)2}/2m^{(k)})$  for species  $k$ . Thus, for a given  $A$ , each species has a different critical radius  $r_*^{(k)}$ . It can thus be expected that the size of the central void should be mainly determined by the grains with the smallest  $r_*$ . One can see this effect in Fig. 1. For example, in Figs. 1 (a4), (b4), (c4), and (d4), when  $A=5$ , the size of the central void is determined by the radius  $r_*^{(2)}$  and it decreases with increasing  $m^{(2)}$ , since  $r_*^{(2)} < r_*^{(1)}$  with  $m^{(2)} > m^{(1)}$ . The exact size of the central void is also affected by grains with larger  $r_*$ , since all the grains are interacting with each other. We also can see that at the given  $m^{(1)}$ ,  $q^{(1)}$ ,  $m^{(2)}$ , and  $q^{(2)}$ , for example, as shown in Figs. 1 (b1), (b2), (b3), and (b4),  $r_*^{(2)}$  increases with  $A$  and is

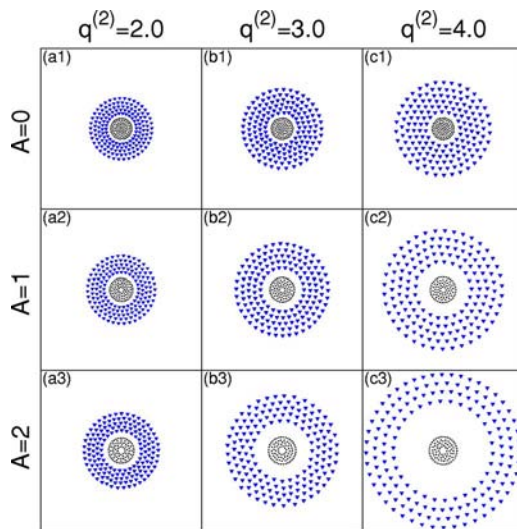


FIG. 3. (Color online) Calculated minimum-energy configurations for two-species grains of the same mass but different charges. The total number of grains is  $N=250$ . The numbers of grains of species 1 (circles) and 2 (triangles) are  $N^{(1)}=89$  and  $N^{(2)}=161$ , respectively.

smaller than  $r_*^{(1)}$ , and therefore the size of the central void also increases with  $A$ . However, the locations of the species-1 and species-2 shells cannot be deduced from the critical radii  $r_*^{(1,2)}$ . For example, in Figs. 1 (a1), (b1), (c1), and (d1), for  $A=0$ ,  $r_*^{(1)}=r_*^{(2)}=0$  and there is no central void in the system, no matter how the value of  $m^{(2)}$  changes, but the grains with the larger (smaller) mass are located near to (far away from) the center of the system. The steady-state locations of the different shells are determined by minimization of the total potential energy of the system. Thus, one can only qualitatively predict the relative size of the central void from  $A$  and  $m^{(2)}$  by calculating the critical radii  $r_*^{(k)}$ . From Figs. 1 (b4), (c4), and (d4), we also can see that the species-1 shell is bounded by perfect outer and inner rings with rather high density, and in between lower-density rings are found. In fact, the grains in the lower-density rings came from an earlier single ring through zig-zag transitions as discussed by Schweigert *et al.*<sup>26</sup> The details and conditions for the zig-zag transitions will be discussed in a future work.

Thus, in a two-species system, both band and center circular voids can appear and coexist. This is in contrast to a single-species system, where only a center void can occur. The obtained minimum-energy configurations are in good qualitative agreement with the cross sections of the 3D structures observed by Huang *et al.*<sup>14</sup>

## 2. Different charge

Band and center voids can also appear if the grain species have the same mass but different charge. Figure 3 shows typical calculated minimum-energy configuration of a two-species system ( $N=250$ ) in which the grains have the same mass but different charge. The subfigures (all of the same arbitrary scale) are arranged such that the columns show the effect of the drag force, and the rows show the effect of the relative charge  $q^{(2)}$ . From Fig. 3, one can see that the grains again organize themselves into two shells, with those of the

smaller charge near the center of the trap. This is because at a given  $A$ , grains with larger charge experience a stronger outward drag force. Again, here the repulsive Coulomb interaction prevents the grains from coming too close together. It follows that the grains of different charge are separated, with those of a larger charge further away from the center than those with a smaller charge. Moreover, from Fig. 3 one can also see that at a given  $q^{(2)}$ , with increasing  $A$  the overall size of the dust system and the band void between the dusty regions become larger, and a void at the center of the trap appears and grows, since the grains experience a stronger outward drag force. From the first row in Fig. 3, we can also see that for  $A=0$ , there is no central void in the system, but with increasing  $q^{(2)}$ , the system size increases, and the sizes of the band void and the species-1 shell are almost unaffected. This can be explained as follows. At  $A=0$  the grains only experience the charge-dependent interparticle repulsive Coulomb (with an attractive component) and the quadratic confinement forces. The Coulomb interaction tends to expand the grain system, which then becomes larger. However, the species-1 grains are not affected by the increase of  $q^{(2)}$ , so that the size of the corresponding shell remains almost unchanged. That is, in Fig. 3, the system size is determined by the shell of grains species 2. Finally, one can also see that when  $A \neq 0$ , with increasing  $q^{(2)}$ , the sizes of the overall system as well as of the band void increase rapidly. This is due to the drag as well as the Coulomb repulsive forces acting on the grains. With increasing  $q^{(2)}$ , the grains of species 2 experience a stronger outward drag force as well as the repulsive interaction pushing the grains apart, leading to a rapid increase of the size of the species-2 shell with  $q^{(2)}$ . The species-1 grains remain unaffected by the increase of  $q^{(2)}$ , so that the sizes of the corresponding shell as well as the center void are unaffected by increase of  $q^{(2)}$ . However, the band void between the species-1 and species-2 shells increases with  $q^{(2)}$ , since the species-2 shell expands outwards with  $q^{(2)}$ .

We can also understand the variation of the central-void size with  $q^{(k)}$  and  $A$  from the expression for the critical radii  $r_*^{(k)}=A(q^{(k)2}/2m^{(k)})$ , where  $k=1,2$ . For example, in Figs. 3 (a3), (b3), and (c3), for a given  $A=2$ , with increasing  $q^{(2)}$ , the critical radius  $r_*^{(1)}$  is a constant and smaller than  $r_*^{(2)}$ , so that the size of the central void is also almost unaffected by  $q^{(2)}$ . The variation of the central-void size with  $A$  at a given  $q^{(2)}$  can also be explained in the same manner. That is, the size of the central void is determined mainly by the grains with the smallest critical radius.

## 3. Different mass and charge

Figure 4 shows typical calculated minimum-energy configurations of a two-species system ( $N=250$ ) in which the species have different mass and charge. Again, the subfigures are all of the same arbitrary scale and are arranged such that the columns show the effect of the drag force, and the rows show the effect of the relative charge  $q^{(2)}$  and mass  $m^{(2)}$ . Figure 4 (a1) shows that with  $A=0$ , when the two-species grains have the same mass-to-charge ratio, the grains are indistinguishable despite the fact that they have different

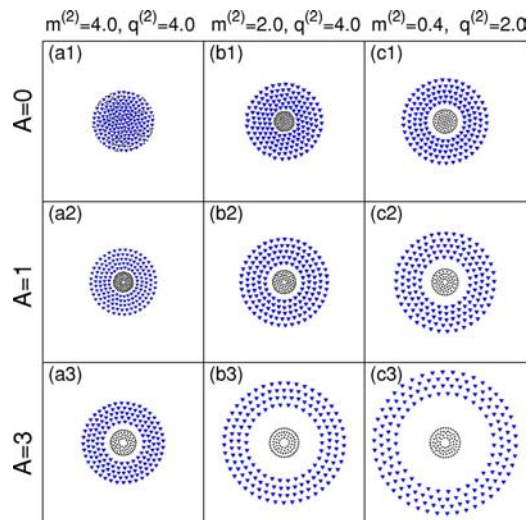


FIG. 4. (Color online) Calculated minimum-energy configurations for two-species grains of different masses and charges. The total number of grains is  $N=250$ . The numbers of grains of species 1 (circles) and 2 (triangles) are  $N^{(1)}=89$  and  $N^{(2)}=161$ , respectively.

mass and charge. However, for  $A=0$  but different mass-to-charge ratios, one can see from Figs. 4 (b1) and (c1) that the species are grouped in two shells, with that of the larger mass-to-charge ratio occupying the center region of the trap. This is due to a balance between the mass-dependent confinement force and the charge-dependent interparticle forces. Moreover, the first row of Fig. 4 shows that even for  $A=0$  the band void can appear if the two mass-to-charge ratios are distinct, although no center void appears, regardless of how the mass-to-charge ratios are varied. One can also see from Figs. 4 (a2) and (a3) that for  $A \neq 0$ , the two species are still separated into two shells although all the grains have the same mass-to-charge ratio. This is expected since the drag force is only charge dependent. From Fig. 4, it is also clear that at any given  $m^{(2)}$  and  $q^{(2)}$ , with increasing  $A$ , the band as well as the center void will appear. The size of both types of voids increases with  $A$ . At any given  $A$ , the size of the complete system as well as the band void between the species-1 and species-2 shells increase with decreasing species-2 mass-to-charge ratio, since the latter grains experience relatively less confinement force and more interparticle repulsive and outward drag forces that push them away from the center of the trap. The forces on the species-1 grains again remain unchanged, so that the center void is also not changed by the species-2 mass-to-charge ratio. That is, the system size is determined mainly by the size of the species-2 shell. From Fig. 4, we can see that the size of the central void is still mainly determined by the grains with the smallest critical radius among the radii of  $r_*^{(k)}$ .

## B. System with four-species of grains

From the above subsection we can conclude that in a two-species system a band-like void and a circular void can coexist in the presence of an external drag force, no matter what the mass and charge of the two species are. However, in their dusty plasma experiments Huang *et al.*<sup>14</sup> also observed

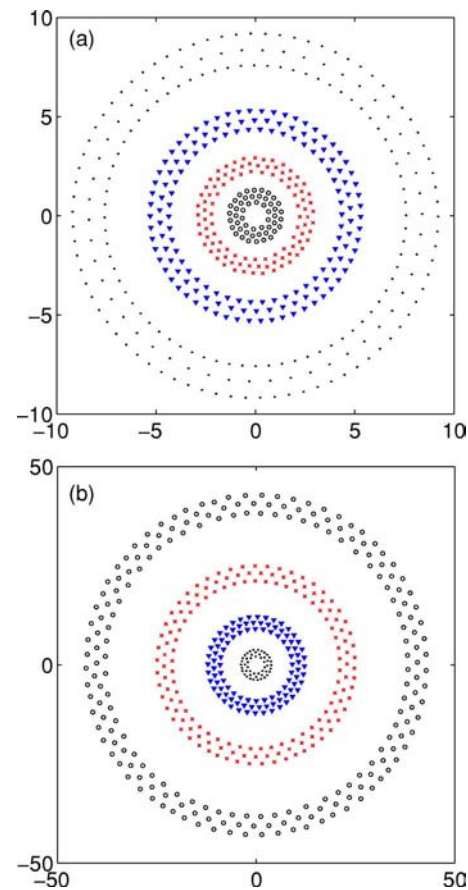


FIG. 5. (Color online) Calculated minimum-energy configurations for four-species grains. The grains of species 1, 2, 3, and 4 are denoted by dots, triangles, crosses, and open circles, respectively. In (a), the grains have the same charge but different masses,  $N=500$ ,  $N^{(1)}=200$ ,  $N^{(2)}=150$ ,  $N^{(3)}=100$ ,  $N^{(4)}=50$ ,  $m^{(2)}=2$ ,  $m^{(3)}=4$ ,  $m^{(4)}=8$ , and  $A=10$ ; In (b), the grains have the same mass but different charges,  $N=500$ ,  $N^{(1)}=50$ ,  $N^{(2)}=100$ ,  $N^{(3)}=150$ ,  $N^{(4)}=200$ ,  $q^{(2)}=2$ ,  $q^{(3)}=3$ ,  $q^{(4)}=4$ , and  $A=5$ .

multiple concentric band voids. From the above results, we can speculate that the latter might be caused by the presence of multiple species of grains, as can be expected during the various stages of dust formation and growth.<sup>14</sup>

Accordingly, we now consider the minimum-energy configurations of a larger system ( $N=500$ ) with four species of grains. Figure 5 shows the typical calculated minimum-energy states of a system with four species of grains having the same charge but different masses [Fig. 5(a)] and having the same mass but different charges [Fig. 5(b)]. As expected from the preceding results, the different species are separated into different shells with concentric band voids in between. In both cases, a center void is also found. Moreover, in Fig. 5(a), grains with larger mass are located closer to the trap center, and in Fig. 5(b), grains with smaller charge are located closer to the center. We have also investigated much larger systems with more grains and species. The results show that the central as well as the band voids appear for most parameter ranges. The grains of the same species tend to populate a common shell, and the maximum number of possible shells formed of the different grains equals to the number of different species in the system.

#### IV. CONCLUSION

Two-dimensional systems of multispecies charged grains interacting through long-range repulsion and short-range attraction forces confined in a quadratic trap in the presence of an external radially outward drag force have been studied. The minimum-energy configurations are investigated by MD simulation. It is found that the drag force can lead to the appearance of disk- and band-like voids separating grains of different mass and charge. The size of the central disk-like void is mainly determined by the grains with the smallest critical radius at which the particles have their minimal external potential energy. The maximum number of possible shells formed of the different grains equals to the number of different species in the system.

The occurrence of band voids should be quite common in 2D plasmas containing more than one species of dust grains. The center void will appear if the drag force is sufficiently strong. Even when there is no attraction between the grains ( $B=0$ ), similar configurations still can be obtained. But the system size will be larger, the density of the shells lower, and the size of the central and band voids smaller (compared to that for  $B \neq 0$ ). As expected, the attractive interparticle force makes the shells denser, but does not otherwise affect the system structuring. Qualitatively, the void structures agree well with that found in the horizontal slices of the 3D structures obtained in the observations.<sup>14</sup> In the experiments,<sup>14</sup> the discharge is not symmetric in the vertical direction and the dust structures are 3D. The voids appear as domes and/or nested dome-shaped shells with their bottoms adjacent to the bottom electrode. However, our results should be applicable to the horizontal cross sections since the dynamic horizontal force balance process remains the same as in the 2D case. It should also be pointed out that in a 3D system containing well developed dust grains, grains with different mass and charge will probably be localized in different 2D planes. However, in the problem of interest here, the dust grains are still in their evolving stage. They are extremely fine (submicrometer) and weakly charged. In fact, in the experiments,<sup>14</sup> under an optical microscope the grains appear and behave like a light-scattering gas cloud rather than individual particles. It can be expected that the grains with similar mass and charge may stay close together vertically in a layer with small (say much smaller than the diameter of the layer) thickness. Thus the results of the 2D simulation should be qualitatively applicable to horizontal cross section of the 3D shells observed in the experiments. On the other hand, the 2D results may not correctly predict the phase structure of the dusty regions, since the latter also depends on packing order which is associated with energy minimization of the entire 3D system.

We can conclude that within the limitations of available experimental data and validity of our theoretical model, the results here agree qualitatively with the experimental findings.<sup>14</sup> A more quantitative comparison with the experiments is possible only when the dust charge and mass distributions in the plasma can be measured. Furthermore, the

effective local electric field may deviate from the quadratic trapping potential because of plasma transport.<sup>11</sup> On the other hand, our results may be useful as a guide to future experiments specifically designed for investigating the mass, charge and size effects on void structures.

The present result is another example that under appropriate conditions dusts of different species can separate.<sup>27,28</sup> Such a phenomenon should be useful for diagnostics of dust particle growth, obtaining information on a dusty plasma system (namely by adding to it new species of dust grains), separation of nanoparticles and isotopes, as well as in industrial applications. It should also be helpful in improving the theoretical modeling of complex plasmas.

#### ACKNOWLEDGMENTS

Y. H. Liu acknowledges a GOA project of the University of Antwerp for financial support and the National Science Foundation of China (Project No. 10205025) for initializing this work. Y. H. Liu and Z. Y. Chen would also like to thank a Bilateral Project between Flanders and China for financial support.

<sup>1</sup>G. Praburam and J. Goree, Phys. Plasmas **3**, 1212 (1996).

<sup>2</sup>R. Samsonov and J. Goree, Phys. Rev. E **59**, 1047 (1999).

<sup>3</sup>R. P. Dahiya, G. V. Paeva, W. W. Stoffels, E. Stoffels, G. M. W. Kroesen, K. Avinash, and A. Bhattacharjee, Phys. Rev. Lett. **89**, 125001 (2002).

<sup>4</sup>G. E. Morfill, H. M. Thomas, U. Konopka, H. Rothermel, M. Zuzic, A. Ivlev, and J. Goree, Phys. Rev. Lett. **83**, 1598 (1999).

<sup>5</sup>J. Goree, G. E. Morfill, V. N. Tsytovich, and S. V. Vladimirov, Phys. Rev. E **59**, 7055 (1999).

<sup>6</sup>V. N. Tsytovich, S. V. Vladimirov, G. E. Morfill, and J. Goree, Phys. Rev. E **63**, 056609 (2001).

<sup>7</sup>N. D'Angelo, Phys. Plasmas **5**, 3155 (1998).

<sup>8</sup>A. V. Ivlev, D. Samsonov, J. Goree, G. Morfill, and V. E. Fortov, Phys. Plasmas **6**, 741 (1999).

<sup>9</sup>K. Avinash, Phys. Plasmas **8**, 351 (2001).

<sup>10</sup>X. Wang, A. Bhattacharjee, S. K. Gou, and J. Goree, Phys. Plasmas **8**, 5018 (2001).

<sup>11</sup>I. Denysenko, M. Y. Yu, L. Stenflo, and N. A. Azarenkov, Phys. Plasmas **12**, 042102 (2005).

<sup>12</sup>M. Kretschmer, S. A. Khrapak, S. K. Zhdanov *et al.*, Phys. Rev. E **71**, 056401 (2005).

<sup>13</sup>M. R. Akdim and W. J. Goedheer, Phys. Rev. E **65**, 015401 (2001).

<sup>14</sup>F. Huang, M. F. Ye, L. Wang, and N. Jiang, Chin. Phys. Lett. **21**, 121 (2004).

<sup>15</sup>V. N. Tsytovich and G. E. Morfill, Plasma Phys. Rep. **28**, 171 (2002).

<sup>16</sup>Y. P. Chen, H. Luo, M. F. Ye, and M. Y. Yu, Phys. Plasmas **6**, 699 (1999).

<sup>17</sup>K. Nelissen, B. Partoens, and F. M. Peeters, Phys. Rev. E **71**, 066204 (2005).

<sup>18</sup>C. Reichhardt, C. J. Olson Reichhardt, I. Martin, and A. R. Bishop, Phys. Rev. Lett. **90**, 026401 (2003).

<sup>19</sup>C. J. Olson Reichhardt, C. Reichhardt, and A. R. Bishop, Phys. Rev. Lett. **92**, 016801 (2004).

<sup>20</sup>V. M. Bedanov and F. M. Peeters, Phys. Rev. B **49**, 2667 (1994).

<sup>21</sup>V. A. Schweigert and F. M. Peeters, Phys. Rev. B **51**, 7700 (1995).

<sup>22</sup>J. A. Drocco, C. J. Olson Reichhardt, C. Reichhardt, and B. Jankó, Phys. Rev. E **68**, 060401 (2003).

<sup>23</sup>K. Nelissen, B. Partoens, and F. M. Peeters, Phys. Rev. E **69**, 046605 (2004).

<sup>24</sup>M. Kong, B. Partoens, and F. M. Peeters, Phys. Rev. E **65**, 046602 (2002).

<sup>25</sup>F. Huang, M. F. Ye, L. Wang, and N. Jiang, Chin. Phys. **13**, 1896 (2004).

<sup>26</sup>I. V. Schweigert, V. A. Schweigert, and F. M. Peeters, Phys. Rev. B **54**, 10827 (1996).

<sup>27</sup>H. Luo and M. Y. Yu, Phys. Fluids B **4**, 3066 (1992).

<sup>28</sup>J. X. Ma, J. Y. Liu, and M. Y. Yu, Phys. Rev. E **55**, 4627 (1997).